

# Magnitude clustering and dynamical scaling in trigger models for earthquake forecasting

Eugenio Lippiello,<sup>1</sup> Cataldo Godano<sup>2</sup> and Lucilla de Arcangelis<sup>3</sup>

<sup>1</sup> *Physics Department and CNISM, University of Naples "Federico II", 80125 Napoli, Italy*

<sup>2</sup> *Department of Environmental Sciences and CNISM,  
Second University of Naples, 81100 Caserta, Italy*

<sup>3</sup> *Department of Information Engineering and CNISM,  
Second University of Naples, 81031 Aversa (CE), Italy*

One of the main interests in seismology is the formulation of models able to describe the clustering in time occurrence of earthquakes. Analysis of the Southern California Catalog shows magnitude clustering in correspondence to temporal clustering. Here we propose a dynamical scaling hypothesis in which time is rescaled in terms of magnitude. This hypothesis is introduced in the context of a generalized trigger model and gives account for clustering in time and magnitude for earthquake occurrence. The model is able to generate a synthetic catalog reproducing magnitude and inter-event time distribution of thirty years California seismicity.

PACS numbers: 64.60.Ht,91.30.Dk,89.75.Da

The great interest in the study of earthquake occurrence is linked to the challenge of predicting the time, the location and the energy of the next earthquake. The energy release  $E$  in a seismic event can be expressed by the magnitude  $M$  via the logarithm relation  $M \propto \log E$  [1], and the magnitude distribution is described by an exponential law usually referred as the Gutenberg-Richter (GR) law [2]  $P(M) \sim 10^{-bM}$ , where  $b$  is a parameter close to one. The logarithm relation leads to a power law behaviour for the energy distribution, which is generally the signature of critical phenomena.

It is widely observed that earthquakes tend to occur in bursts. These bursts start immediately following a large main event, giving rise to the main-aftershock sequences, described by the Omori law [3]. This states that the number of aftershocks  $n(t)$  decays in time as  $n(t) \sim (t+c)^{-p}$  where  $p$  is generally close to 1 and  $c$  is an initial time introduced in order to avoid the divergence at  $t=0$ . The most important implication of this law is that we cannot assume a Poissonian occurrence for earthquakes, namely characterized by a constant rate of occurrence, but rather a clustered one.

Another signature of non-Poissonian behaviour for earthquake occurrence is the complex distribution of the inter-occurrence times between two successive events. In fact, for a Poissonian process, this distribution would be an exponential whereas experimental data exhibit a more complex behaviour [4]. Moreover, one can compute the intertime distribution  $D(\Delta t, M_L)$  where  $\Delta t$  is time distance between successive events occurred inside a finite geographic region and with magnitude greater than a given threshold  $M_L$ . Indicating with  $P_C(M)$  the cumulative magnitude distribution inside the considered region, one observes [4, 5]

$$D(\Delta t, M_L) = P_C(M_L) f(P_C(M_L) \Delta t) \quad (1)$$

where  $f$  is a universal function, independent on  $M_L$  and on the geographical region. The observed universality is a further signature of criticality and indicates that  $D(\Delta t, M_L)$  is an appropriate quantity to characterize the temporal clustering of earthquakes.

A widely used approach to earthquakes clustering is provided by "trigger models" [6]. These assume a Poissonian occurrence of triggering events, whereas the occurrence of the "triggered" earthquakes is described in terms of a correlation function with previous events. Among the trigger models the Epidemic Type Aftershocks Sequence (ETAS), introduced by Kagan-Knopoff [7] and developed by Ogata [8], describes mainshocks and aftershocks on the same footing. More precisely, each earthquake can generate "its own aftershocks" and furthermore the number of these aftershocks depends exponentially on the magnitude of the "main". The model has been deeply investigated analytically and numerically [9].

In this paper we are interested in the description of temporal evolution of seismic activity. For this reason we neglect spatial dependencies and treat seismicity as a stochastic process  $M_i(t_i)$ , where  $M_i$  is the magnitude of the  $i$ -th earthquake occurred at time  $t_i$  inside a large but finite geographic region. The process is defined by the conditional probability density  $p(M(t)|\{M_i(t_i)\})$  to have an earthquake of magnitude  $M$  at time  $t$  given the history of past events  $\{M_i(t_i)\}$ . Here we consider a generalized version of the trigger model by Vere-Jones

$$p(M(t)|\{M_i(t_i)\}) = \sum_{i:t_i < t} p(M(t)|M_i(t_i)) + \mu P(M) \quad (2)$$

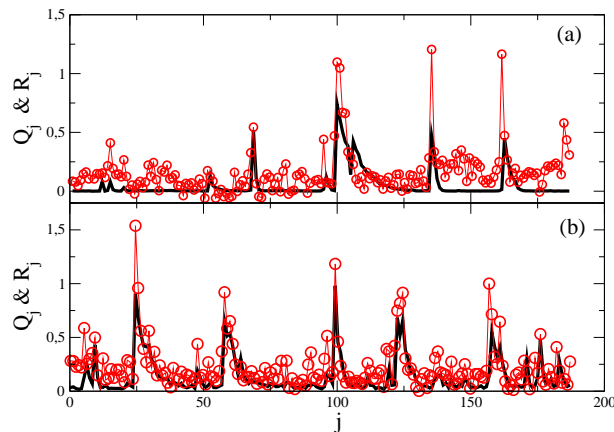


FIG. 1: (Color online) (a) Experimental distributions of the quantities  $Q_j$  (red  $\circ$ ) and  $R_j$  (black continuous line) for the California Catalog.  $R_j$  is measured in unit of  $(6\text{hours})^{-1}$  and in order to improve the comparison  $Q_j$  is vertically shifted by the constant amount  $-1.5$ . Peaks for  $R_j$  indicate main-after shock sequences. (b) Numerical distributions of  $Q_j$  and  $R_j$  from Eq.(7).

where  $p(M(t)|M_i(t_i))$  is the "two-point" conditional probability density,  $\mu$  is a Poissonian rate and the magnitude distribution  $P(M) \sim 10^{-bM}$  obeys the GR law. Different forms of  $p(M(t)|M_i(t_i))$  correspond to different models for seismicity. In the ETAS model one assumes [8]

$$p(M(t)|M_i(t_i)) = P(M)g(t - t_i; M_i) \quad (3)$$

where the propagator  $g(t - t_i; M_i) \propto 10^{\alpha M_i} (t - t_i + c)^{-p}$ . In order to have a normalized probability one must impose  $p > 1$ . Moreover, if  $\alpha \geq b$  the model presents finite time singularity unless one assumes a large magnitude cut-off [10]. Alternatively, one must take  $\alpha < b$  as supported by some experimental observations [11].

A strong assumption of the ETAS model is the factorization in Eq.(3), which states that the magnitude of an earthquake is completely independent on the magnitudes and times of occurrence of previous events. In order to test this assumption with real seismic data, we observe that the quantity  $P_C(M_L) \sim 10^{-bM_L}$  takes the role of a characteristic time scale in Eq.(1). Hence, if one considers a subset of  $N$  events, the quantity  $Q = N/[\sum_i 10^{-bM_i}]$  can be related to the rate of occurrence  $R = N/[\sum_i (t_i - t_{i-1})]$ , where the sum is inside the chosen subset. To this extent, we divide data recorded in the Southern California Catalog (1975-2004) [12] in subsequent sets of 200 events with  $M \geq 2.5$  and we compute the quantities  $Q_j$  and  $R_j$  inside the  $j$ -th subset. If the magnitude distribution were constant in time, as supposed in Eq. (3),  $Q_j$  should fluctuate around an average value. Conversely, the experimental  $Q_j$  displays scattered and narrow peaks (Fig.1a). Interestingly, these peaks are closely located to peaks in the  $R_j$  distribution. It is well known that peaks of  $R_j$  are located soon after main-shocks and indicate the presence of main-after shock sequences. Fig.1a, then, shows that in subsets of the catalog where activity has an higher rate, the probability to have large magnitude events is also raised. This aspect can be directly investigated by computing the cumulative magnitude distribution  $P_C(M)$  only inside the ensemble of main-aftershock sequences. Considering only sequences with main-shock magnitude  $M \geq 6$ , one obtains that  $P_C(M)$  exhibits a GR behaviour with a best fit  $b$ -value  $b = 0.75$ , lower than the  $b$ -value obtained for the whole catalog ( $b = 0.95$ ) within the 95% significativity level. This result further supports the idea that large earthquakes not only produce the clustering in time described by the Omori law, but also a clustering in magnitude. The ETAS model does not take into account this last physical mechanism.

In order to include the magnitude clustering within a trigger model approach, we propose a dynamical scaling hypothesis: the magnitude difference  $M_i - M_j$  fixes a characteristic time scale  $\tau_{ij} = k10^{\frac{b}{p}(M_j - M_i)}$  so that the conditional probability is magnitude independent when times are rescaled by  $\tau_{ij}$  and  $k$  is a constant measured in seconds

$$p(M_i(t_i)|M_j(t_j)) = F \left[ \frac{(t_i - t_j)}{\tau_{ij}} \right] \quad (4)$$

Let us then consider the probability to have an event of magnitude  $M$  at time  $t$  given a triggering event at time  $t_0$  of arbitrary magnitude  $M_0$ ,  $p(M, t - t_0) = \int dM_0 P(M, t|M_0, t_0)P(M_0)$ . Assuming the GR law for  $P(M_0)$  and using

Eq.(4), one finds

$$p(M, t - t_0) = \frac{10^{-bM}}{(t - t_0)^p} \int_0^{10^{bM}(t-t_0)^p} F(z^{1/p}) dz. \quad (5)$$

From this equation we obtain both the GR and Omori law independently of the specific form of  $F(z)$  provided that the appropriate constraints are imposed at small and large  $z$ . In fact, assuming that the conditional probability (6) is maximal soon after the triggering event, must be  $F(0) > 0$ . Furthermore, in order to have normalized distributions, the conditional probability must decay to zero for large time separation and a constraint on the behaviour of  $F(z^{1/p})$  must be imposed at large  $z$ , namely a decay faster than  $1/z$ . Because of this constraints, the integral in the rhs of Eq.(5) is a constant for large  $t - t_0$ , and the GR and Omori law directly follows from Eq.(4). The above observation suggests that statistical features of the trigger model can be independent on the detailed form of  $F(z)$  once the scaling Eq.(4) is assumed. This hypothesis together with the relationship between numerical and experimental behaviour can be directly tested in numerical simulations.

In a numerical protocol one assumes at initial time  $t_0 = 0$  a single event of arbitrary magnitude chosen in a fixed range  $[M_{min}, M_{max}]$ . Time is then increased of a unit step  $t = t_0 + 1$ , a trial magnitude is randomly chosen in the interval  $[M_{min}, M_{max}]$  and Eq.(2) gives the probability to have an earthquake in the time window  $(t_0, t_0 + 1)$ . If this probability is larger than a random number between 0 and 1, an earthquake takes place, its magnitude and time of occurrence are stored and successively used for the evaluation of probability for future events. Time is then increased and in this way one constructs a synthetic catalog of  $N_e$  events. The term  $\mu$  in Eq.(2) represents an additional source of earthquakes Poissonian distributed in time with a magnitude chosen from the GR distribution with  $b = 0.8$ .

Following this protocol, we generate sequences of 15000 events using a power law form for  $F(z)$

$$F(z) = \frac{A}{z^\lambda + \gamma} \quad (6)$$

and then we compute the numerical distributions  $D(\Delta t, M_L)$  and  $P(M)$ . These distributions are compared with the experimental data from the Southern California Catalog. For different values of  $\lambda$ , it is always possible to find a set of parameters  $A, \gamma, b/p, \mu$  such that numerical data reproduce, on average, the statistical features of earthquake occurrence both in time and in magnitude. The parameter  $k$  is fixed a posteriori in order to obtain the collapse between numerical and experimental data.

In Fig.2 we plot the experimental and numerical  $D(\Delta t, M_L)$  considering two different values of  $\lambda$  ( $\lambda = 1.2$  and  $5$ ) and  $M_L$  ( $M_L = 1.5$  and  $2.5$ ). In the inset we also present the magnitude distributions. Data for different values of the parameters follow a universal curve and the same collapse is obtained for other values of  $\lambda > 1$ . The accordance between experimental and numerical curves indicates that the hypothesis of dynamical scaling is able to reproduce two fundamental properties of seismic occurrence, namely the GR law and Eq. (1), independently of the details of  $F(z)$  [13].

The ETAS model is a particular case of Eq.(6) corresponding to  $\gamma = 0$  and  $\lambda \simeq 1$ . We want to stress the important difference due to the presence of a non-zero  $\gamma$ . From a mathematical point of view, the constant  $\gamma$  avoids the finite time singularity of the ETAS model with  $\alpha = b$  discussed previously [9]. From a physical point of view, the constant  $\gamma$  gives rise to the observed clustering in magnitude. Indeed, for a given mainshock of magnitude  $M_j$  at time  $t_j$ , at each time ( $t_i > t_j$ ) it is possible to define a sufficiently large magnitude difference  $\Delta M$  such that, if  $M_j - M_i > \Delta M$ , we have that  $z^\lambda$  is negligible with respect to  $\gamma$  and therefore  $F[(t_i - t_j)/\tau_{ij}] \simeq A/\gamma$ . In other words after a large event, small earthquakes tend to be equiprobable.

We have also performed more extensive simulations using a different expression for  $F(z)$

$$F(z) = \frac{A}{e^z - 1 + \gamma} \quad (7)$$

Eq.(7) states that two events of magnitude  $M_i$  and  $M_j$  are correlated over a characteristic time  $\tau_{ij}$  and become independent when  $t_i - t_j > \tau_{ij}$ . As a consequence only a small fraction of previous events can affect the probability of future earthquakes so that, after a certain time, Earth crust loses memory of previous seismicity. This aspect is perhaps more realistic with respect to the idea, contained in a power law correlation, that events are all correlated with each other and also gives rise to important implications for seismic forecasting. The construction of seismic catalogs, indeed, dates back to about 50 years, and according to Eq.(7) one can have good estimates of seismic hazard without considering previous seismicity. This is no longer true if one assumes a power law time decorrelation of the type (6) especially for small values of  $\lambda$ . We want also to point out that a general state-rate formulation [15] gives rise

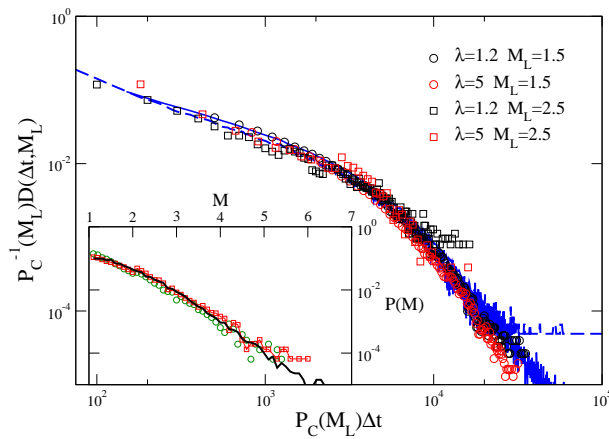


FIG. 2: (Color online) The intertime distribution obtained using Eq. (6), with two different values of  $\lambda = 1.2, 5$  and  $M_L = 1.5, 2.5$ . Continuous and broken curve are the experimental  $D(\Delta t, M_L)$  with  $M_L = 1.5$  and  $M_L = 2.5$  respectively. For  $\lambda = 1.2$  we set  $k = 210 \text{sec}$ ,  $A = 1.410^{-4} \text{sec}^{-1}$ ,  $\mu = 410^{-7}$ ,  $\gamma = 1$ . For  $\lambda = 5$  we set  $k = 420 \text{sec}$ ,  $A = 1.910^{-4} \text{sec}^{-1}$ ,  $\mu = 1.510^{-6}$ ,  $\gamma = 0.1$ . In the inset the magnitude distribution of the experimental catalog (black line) and numerical catalog with  $\lambda = 1.2$  (red  $\circ$ ) and  $\lambda = 5$  (green  $\square$ ).

to correlations between earthquakes that decay exponentially in time. We finally observe, that taking into account only a fraction of previous events in the evaluation of conditional probabilities, the numerical procedure considerably speeds up. In the case of long temporal correlation CPU time grows with the number of events as  $N_e^2$ , whereas in the case of an exponential tail the growth is linear in  $N_e$ . For this reason, assuming the functional form (7) one can simulate very large sequences of events. In particular for a different choice of parameters, one can construct synthetic catalogs containing the same number of events ( $N_e = 245000$  with  $M \geq 1.5$ ) of the experimental California Catalog. In fig. 3 we compare numerical and experimental distributions  $D(\Delta t, M_L)$  for three different values of  $M_L$ . For each value of  $M_L$ , the numerical curve reproduces the experimental data and obviously fulfill Eq.(1) (inset (a) in Fig.(3)). Also the numerical magnitude distribution  $P(M)$  is in very good agreement with the experimental one (inset (b) in Fig.(3)). Finally, evaluation of quantities  $Q_j$  and  $R_j$  for the synthetic catalog leads, as expected, to the same clustering behaviour as for experimental data (Fig.1b). After fixing  $k$ , we express numerical time unit in seconds and we observe that numerical catalog corresponds to a period of about  $9.9 * 10^9 \text{sec} \simeq 30$  years. Therefore our model is able to construct a synthetic catalog covering about 30 years that contains about the same number of events and displays the same statistical organization in magnitude and time of occurrence as real California Catalog. The high efficiency of the model in reproducing past seismicity indicates that the model is a good tool for earthquake forecasting. In fact, given a seismic history, Eq.(2) together with Eq.s(4, 7) gives the probability to have an earthquake of magnitude  $M$  at time  $t$  inside a considered geographic region. Our approach is different from the Reasenber-Jones method [16], which is currently used for evaluation of seismic hazard. This method is based on the generalized Omori law that gives for the rate of occurrence of magnitude  $M$  aftershocks,  $P(t, M) = \hat{A}10^{\hat{b}(M-M_M)}(t-t_M+\hat{c})^{-\hat{p}}$ , where  $t_M$  and  $M_M$  are the time of occurrence and magnitude of the main-shock. The starting set of parameters  $(\hat{b}, \hat{p}, \hat{c}, \hat{A})$  is estimated from previous seismic sequences, and then their value is continuously updated as soon as new data become available. However, strong fluctuations in the magnitude distribution observed in Fig.1 suggest that the extrapolated  $\hat{b}$  from the previous subset may not give the correct value to use for event forecasting. Furthermore, one has an improving parameters estimation as the sequence evolves, but at the same time hazard is decreasing. Conversely in our model parameters  $(A, b/p, \gamma)$  are evaluated on the basis of the entire history of 245,000 events leading to a more precise estimation. Nevertheless, due to the stochastic nature of the process, one observes fluctuations of  $\hat{b}$  and  $\hat{p}$  from one sequence to the other (Fig.1b). Our model, furthermore, also allows hazard estimation outside the Omori sequence and therefore long term forecasting.

We finally observe that also spatial distributions of seismic events reveal some kinds of scale invariance [17, 18, 19]. These indicate that also spatial distribution originates from a critical behaviour of the Earth crust suggesting that a dynamical scaling hypothesis as in Eq.(4) can also work if one appropriately introduces spatial dependencies. In this way it would be possible to construct seismic hazard maps.

Acknowledgements. This work is part of the project of the Regional Center of Competence "Analysis and Monitoring of Environmental Risk" supported by the European Community on Provision 3.16. This research was also supported by EU Network Number MRTN-CT-2003-504712, MIUR-PRIN 2004, MIUR-FIRB 2001.

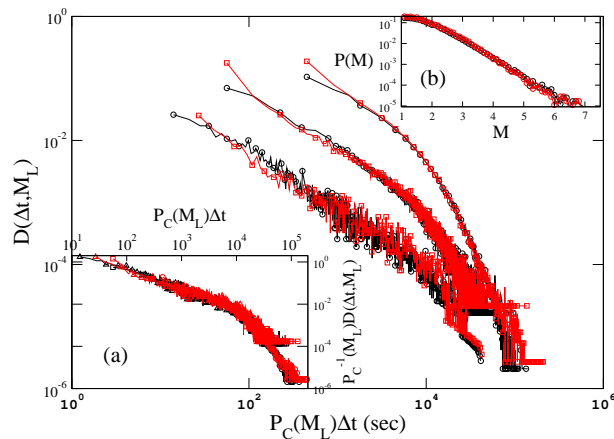


FIG. 3: (Color online) The intertime distribution as a function of  $\Delta t P_C(M_L)$  obtained using Eq.(7) (black circle  $\circ$ ) and compared with the experimental distributions (red  $\square$ ) for three different values of  $M_L$  ( $M_L = 1.5, 2.5, 3.5$ , from top to bottom). We set  $k = 4.9 * 10^4 \text{ sec}$ ,  $A = 6.1 * 10^{-5} \text{ sec}^{-1}$ ,  $\mu = 2 * 10^{-5}$ ,  $\gamma = 0.1$ . In inset (a) the scaling behaviour as in Eq.(1) and in inset (b) the experimental (red) and numerical (black) magnitude distribution.

- 
- [1] H. Kanamori, D.L. Anderson, *Bull. Seize. Soc. Am.* **65**, 1073 (1975).
  - [2] B. Gutenberg, C.F. Richter, *Bull. Seism. Soc. Am.* **34**, 185 (1944).
  - [3] F. Omori, *J. Coll. Sci. Imp. Univ. Tokyo* **7**, 111, (1894).
  - [4] A. Corral, *Phys. Rev. Lett.* **92**, 108501 (2004).
  - [5] P. Bak, K. Christensen, L. Danon and Scanlon T., *Phys. Rev. Lett.* **88**, 178501, (2002)
  - [6] J. F. D. Vere-Jones, *J. Roy. Statist. Soc.*, **B32**, 1, (1970)
  - [7] Y. Y. Kagan and L. Knopoff, *Science* **236**, 1563, (1987)
  - [8] Y. Ogata, *J. Amer. Stat. Assoc.* **83**, 9, (1988)
  - [9] A. Helmstetter and D. Sornette, *Phys. Rev. E* **66** 061104 1, (2002); A. Helmstetter and D. Sornette, *J. Geophys. Res.* **107** 2237, (2002)
  - [10] Y. Y. Kagan, *Geophys. J. Int.* **106**, 123, (1991)
  - [11] A. Helmstetter, *Phys. Rev. Lett.* **91** 058501, (2003)
  - [12] Southern California Seismographic Network, <http://www.scecdc.scec.org/ftp/catalogs/SCSN/>
  - [13] A condition on  $\lambda$  should be imposed from the observation that, taking a single event at  $t = t_0$  and neglecting the Poissonian term in Eq. (2) one obtains a power law  $P(t - t_0) \sim (t - t_0)^{-\lambda p}$ . Hence, one is tempted to fix  $\lambda \simeq 1$  in order to reproduce the Omori law. Nevertheless considering  $\mu > 0$ , also for  $\lambda$  different than one, one can recover Omori law with  $p$  belonging to the experimental range. This observation, for instance, can be indirectly extracted from the short time behaviour of  $D(\Delta t, M_L)$  [14].
  - [14] M.S. Mega *et al.*, *Phys. Rev. Lett.* **90**, 188501 (2003)
  - [15] J.Dieterich, *J. Geophys. Res.* **99**, 2601 (1994)
  - [16] P.A. Reasenber and L.M. Jones, *Science* **243**, 1173 (1989)
  - [17] T.Hirata and M.Imoto, *Geophys. J. Int.* **107**, 155 (1991)
  - [18] J. Davidsen and M. Paczuski, *Phys. Rev. Lett.* **94**, 048501 (2005)
  - [19] C. Godano, and F. Pingue, *Geophys. Res. Lett.* in press